# Detection and Quantitative Measurement of Neuronal Outgrowth in Fluorescence Microscopy Images

Weimiao Yu[a], Hwee Kuan Lee[a], Srivats Hariharan[b], Wenyu Bu[b], Sohail Ahmed[b]

[a]Bioinformatics Institute, #07-01, Matrix, 30 Biopolis Street, Singapore 138671,
[b]Institute of Medical Biology, 8A Biomedical Grove #06-06, Immunos, Singapore 138648

**Abstract.** Automatic and quantitative measurement of neurites is a challenging task, while it is critical in many neurological studies. We developed a fully automatic method to trace and quantitatively measure the neurites. Our measurements are validated by comparison with the semi-automatic NeuronJ and commercial software HCA-Vision. The results demonstrate that the measurements of the three approaches have no significant difference. We also apply our approach for a biological study on neurite outgrowth and the measurements of four different conditions are presented.

## 1 Introduction

Understanding the process of neurite outgrowth and discovering the mechanisms governing neuronal outgrowth are important for neuroregeneration in the treatment of injury and diseases, such as Alzheimer's and Parkinson's diseases. The formation of neuronal circuitry depends on different conditions. High-throughput and high-content image-based screens are powerful tools to discover the conditions that can induce more and longer neurites. In drug discovery, similar screens are applied in order to identify the compounds that induce neuroregeneration. Acquiring high quality and vivid images is only the first step towards a relevant biological conclusion. A biological image contains abundant information, which can only be retrieved with considerable effort. Manually analyzing and measuring these images is subjective, labour intensive and inaccurate. The challenges are how to automatically analyze these images and extract useful information. Detection and quantitative measurements of neuronal outgrowth is a fundamental step in many studies of neuronal development and neuroregeneration. An automatic and quantitative neurite tracing approach is highly desired.

Contributions to this research field come from both biological and computer vision communities. A number of commercial software packages, that can measure the neurite outgrowth are available, such as IN Cell Analyser from GE Healthcare and MetaXpress from MDC. NeruonJ [1], an *ImageJ* plug-in, is a semi-automatic approach to measure the neurites. It helps to reduce manual labour significantly. The user can use the mouse to specify the starting point and the ending point in an image and this software will generate a report of measurements for each image. Another simple-to-use *ImageJ* plug-in for two-dimensional fluorescence images is the NeuriteTracer [2]. This freeware can automatically trace neuronal outgrowth in both complex and simple neuronal cultures. The plug-in performed well on images from three different types of neurons with distinct morphologies. HCA-Vision [3] is a commercial software package, which has a special module for quantifying neurite outgrowth. By using morphological opening, skeletonization and tracing algorithms, this software delivers comprehensive structural information rapidly and reliably. Other works on the neurite tracing tasks are the automatic semantic analysis of neurons [4], labelling and analysis of the neurites [5] and a tracing algorithm of neuron-based assays for high-throughput image screens [6].

In this paper, we present a tracing algorithm to quantitatively measure the neurites. Our package, named *NeuroCyto*, is fully automatic and freely available. Section 2 describes the procedure of image acquisition, segmentation of the cells and how we differentiate the cell bodies and the neurites. Section 3 provides the details of our tracing algorithm. We selected 7 images containing 16 long neurites and used the NeuronJ to manually create the ground truth since the semi-automated approach is very reliable. We provide the comparisons of the measurements between NeuronJ, HCA-Vision and our tracing approach in Section 4. Concluding remarks are presented in Section 5.

## 2 Image acquisition and processing

### 2.1 Cellular image acquisition

This section briefly describes the procedure of image acquisition. N1E115 mouse neuroblastoma cells have been used as a neuronal cell model for a number of years. In our experiment, N1E115 cells were grown on glass coverslip. The cellular images are acquired from fixed N1E115 cells stained by DAPI and FITC- phalloidin. DAPI stains the nucleus, which is blue; FITC-phallodin stains the abundant endogeneous filamentous actin, which is green. The cells

Corresponding author: yuwm@bii.a-star.edu.sg

are counted, seeded and resuspended into monolayer on the coverslips with an appropriate density. The seeding procedure guarantees that nuclei do not overlap with each other. Images were acquired using a wide-field fluorescence microscope with filters for DAPI and FITC stains. The original images were acquired at 20× magnifications with 1366×1020 pixels of 12 bits accuracy. The resolution is 0.31 μm/pixel. Toca-1 is a protein, which can induce the formation of neurites in N1E115 [7]. Cellular images were acquired under four different culture conditions [7]: (I) Serum starvation with 50,000 cells/slide; (II) Serum starvation with 30,000 cells/slide; (III) Toca-1 transfected with 50,000 cells/slide; (IV) Toca-1 transfected with 30,000 cells/slide. More than 1500 images were acquired under each condition. We need to detect the neurites and measure the length quantitatively. Finally, we need to determine under which condition the cells will have more and longer neurites.

### 2.2 Segmentation of the neural cells

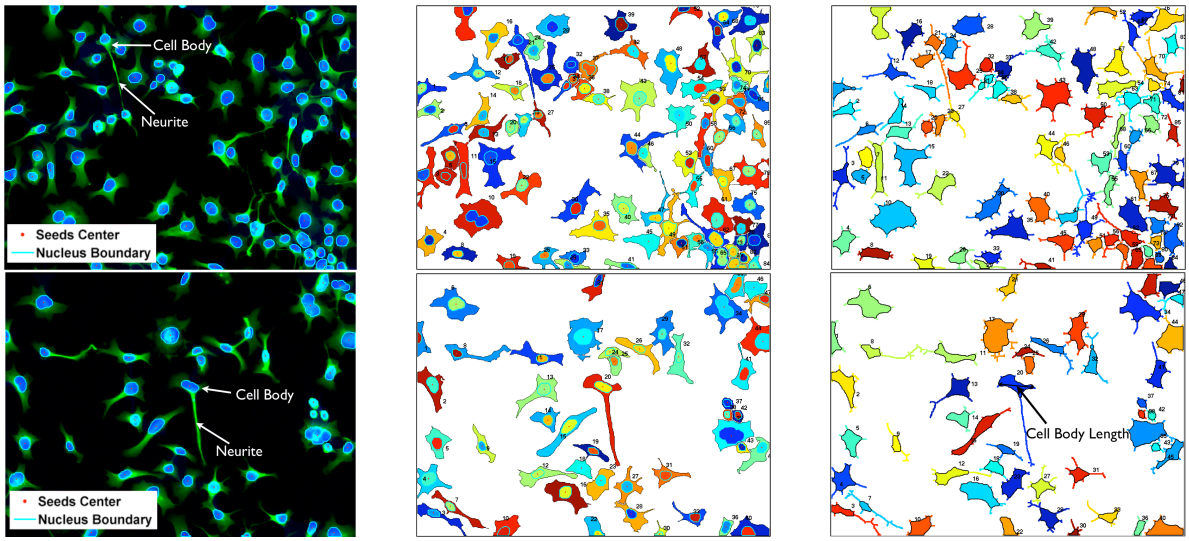


(*a*). Original images (*b*). Segmented images (*c*). Cell bodies and neurites

**Figure 1**. Original cellular image, segmented image and the final result of detected cell bodies and neurites.

Neurites consist of curved line-like structures, as shown in Fig. 1(*a*). In order to obtain the information on a cell-by-cell basis, accurate segmentation is a prerequisite. However, since the cells are clumpy and touch each other, segmentation of the cells is a challenging task. We applied the cellular image segmentation approach based on topological dependence that was recently published in [7, 8]. The source code of this approach is available online[▪]. Due the limitation of space, we can only briefly discuss the parameter selection of the cell segmentation. In the segmentation formulation in [7, 8], $\lambda_1$ and $\lambda_2$ are the weights of foreground and background respectively. The parameters we used are $\lambda_1$=1, $\lambda_2$=50 since we want to emphasis importance of the background such that we may preserve the continuity of weak neurites. In our study, $\Delta t$=10. The detail on how we selected this value is given in [7]. This segmentation approach can segment the clumpy and touched cells, however, it cannot segment the overlapped cells. We randomly select 100 images and manually label the ground-truth for segmentation. In these 100 images, there are only 4.1% overlapped cells in the total cell population. We consider that overlapped cells can be ignored. The segmented cells are shown in Fig. 1(*b*).

### 2.3 Differentiation of cell bodies and neurites

After we segment the cells, we need to distinguish the neurites from the cell body before tracing and measuring. In order to identify the cell bodies, we use the morphological opening operation (erosion followed by dilation) to remove fine structures (neurites) while preserving bulky structures (cell bodies). We applied the opening operation with a deck structure of radius $r_d$ to the segmented images.

| *Opening by* | $r_d$ = 2 | $r_d$ = 5 | $r_d$ = 8 | $r_d$ = 11 | $r_d$ = 15 |
|---|---|---|---|---|---|
| *Accuracy* | 83.5% | 98.89% | 72.70% | 43.58% | 15.42% |

**Table 1**. Accuracy of detected cell bodies using opening by different radius.

We apply a parameter tuning procedure to determine a proper value of the parameter $r_d$. Twenty images were randomly selected. We obtain the cell bodies of these 20 images using $r_d$ = 2, 5, 8, 11 and 14 pixels. Then for each

[▪] http://neuroncyto.bii.a-star.edu.sg/

$r_d$, correctly identified cell bodies are manually counted. The deck structure with radius of 5 pixels achieved the best accuracy, about 99%. Therefore, we use $r_d$ = 5 pixels to differentiate the neurites from the cell bodies. After identifying the cell bodies, we applied the skeletonization [9] to the segmented images and then overlay the cell bodies with the skeletons, as shown in Fig. 1(*c*), thus obtaining the structure of the neurites.

## 3 Automatic neurite tracing

### 3.1 Determination of neurite point status

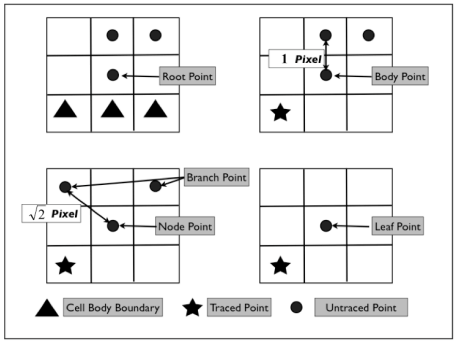


**Figure 2**. Determine the point status based on 3×3 neighbourhood.

As shown in Fig. 1(*c*), the neurites are represented by the skeletons, which are tree-like structures of one pixel width. For the clarity, we call the skeleton pixels "*neurite points*". In order to trace each neurite and measure its length, we first determine the status of the neurite points. We classify the neurite points into five different statuses: root point, body point, node point, branch point and leaf point.

- Root points are neurite points connecting to cell bodies;
- Body points are points which are connected with only two neurite points;
- Node points are where the neurite has branches;
- Branch points are untraced points which are connected to node points;
- Leaf points are the points when the neurite ends,

Determine the status of different points is a labeling problem. Using 3×3 neighborhood, it is trivial to determine the status of each neurite point. Fig. 2 illustrates a few examples how we determine the status of each point.

### 3.2 Tracing and measurement of neurites

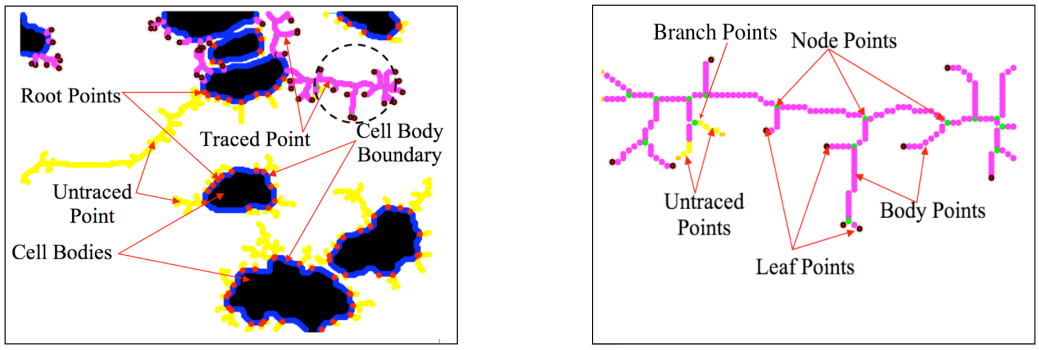


(*a*). Tracing procedure (*b*). Status of each neurite point

**Figure 3**. Illustration of tracing algorithm and the status of the each point.

After we determine the status of each neurite point, an algorithm is developed to automatically trace the neurites and thus measure their lengths. First of all, the algorithm traces around the perimeter of each cell body to find the coordinates of all root points, $\{R_i^x, R_i^y\}$ for $i$=1,2,3…$N$. In our tracing algorithm, we take the root point as a starting point for tracing the corresponding neurite. Let the last traced point be called the current point, therefore in our tracing algorithm, the current point starts from the root point and proceeds towards the leaf points. To trace from the current point to the next point, we look at the status of its neighboring neurite points in a 3x3 window centered at the current point. The next point will be the closest untraced neurite point in this 3x3 window. If there is no such point, then the current point must be a leaf point. When we move to the next point, we record its distance, *e.g.* along the

traced neurite points from the root point and form a directed edge from the current point to the next point. The distance between two adjacent neurite points is 1 pixel if they are four-neighbors and $\sqrt{2}$ pixels otherwise, as shown in Fig. 2. For example, suppose the distance from the root point of the current point is $L$ pixels, then the distance of the next point will be $L$+1 pixels if the next point is a four-neighbor, $L+\sqrt{2}$ pixels otherwise. We continue the tracing until all neurite points are traced. Then the length of the neurite is the largest distance between the root point and the leaf points. The detail of the tracing algorithm is as follow:

*Neurite Tracing Algorithm*

1. For a given cell body, find the all root points around its boundary, *e.g.* $\{R_i^x, R_i^y\}$ $i$=1,2,3…$N$.
2. Select a root point and start tracing. Let the current point be the root point.
3. Let the next point be the closest neurite point within a 3x3 window of the current point.
4. Update the next point's distance from the root point and form a directed edge from the current point to this point. Tracing algorithm depends on the status of the next point:
   i. If it is a body point, set this point to be the current point and go to step 3.
   ii. If next point is a node point, insert the branch points into a buffer (see Fig. 2). Select a new current point from the buffer. Remove this selected point from buffer and go to step 3.
   iii. If next point is a leaf point. Select a new current point from the buffer. Remove this selected point from buffer and go to step 3.
5. If the buffer empty, the tracing of this neurite is completed. Go to step 2, until all the root points are traced.

Our algorithm automatically searches around the boundary of each cell body. When it encounters a neurite root point, it will automatically trace the neurite and quantitatively measure the lengths of its branches. Every traced point will contain the information of its distance from the root point and the point it is being traced from. Fig 3 illustrates the procedure of a neurite tracing using our algorithm. The region within the dashed circle in Fig. 3(*a*) is amplified in Fig. (*b*). Besides the measurement of the neurite lengths, more information can be obtained from this tracing, such as the number of branch points.

### 3.3 Detection of positive cells

Neural cells with a neurite that is at least 1.5 times longer than the cell body length are of special interest in our biological study. The definition of the cell body length is the maximum distance between two points located at the boundary of the cell body. This is illustrated in Fig. 1(*c*). According to the measurement of the neurite length, we report the cells with neurites that are longer than 1.5 times of the cell body length as "positive" cells. We can also calculate the Relative Length (RL) of each neurite, which is defined as the length of the neurite divided by the length of the cell body. A movie, which demonstrated how our tracing algorithm works on a real image and detects the positive cells, is available at http://web.bii.a-star.edu.sg/~yuwm/MIUA2009/Movie_Tracing.mov.

## 4 Experimental results and validation

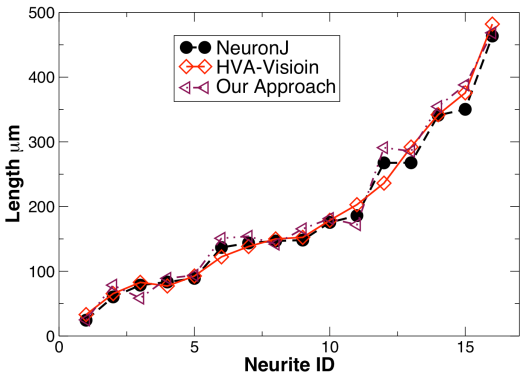


**Figure 4**. Measurements obtained by NeuronJ, HCA-Vision and our approach for 16 neurites in 7 images.

Seven images containing 16 neurites are selected for validating our algorithm. We apply the semi-automated approach NeuronJ to measure the neurites and use its results as our ground truth. We also use HCA-Vision and our approach on the same images. The measurements of the three different approaches are shown in Fig. 4. The images of the tracing results are attached as an Appendix. Comparisons of the three different approaches are shown in Table 2. The relative difference of our approach and HCA-Vision is only 2.7%. HCA-Vision measurements are slightly closer to the NeuronJ results than our measurements. However, the mean differences of all three pair of comparisons are all less than 5%. We can see that the measurements of the neurite length using the three approaches have no

significant differences.

| *Approaches* | *Difference* |
|---|---|
| Our Approach *vs.* NeuronJ | $\mu = \mathbf{4.85\%}$; $\sigma = 2.81\%$ |
| HCA-Vision *vs.* NeuronJ | $\mu = \mathbf{3.20\%}$; $\sigma = 2.74\%$ |
| Our Approach *vs.* HCA-Vision | $\mu = \mathbf{2.70\%}$; $\sigma = 3.87\%$ |

**Table 2**. Relative difference of the measurements obtained by three different approaches.

We make the measurements of all the cells in the images under different conditions. The normalized distributions of the relative neurite length under different conditions are shown in Fig. 5. The dashed line is the 1.5 threshold value to report the positive cells. From the results presented in Fig. 5, we know that Condition III contains more neurites that have longer relative length, *e.g. RL*>3.

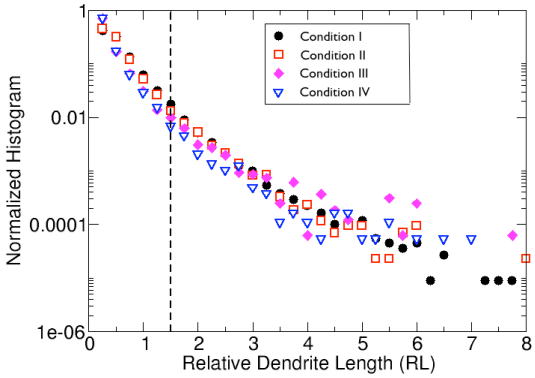


**Figure 5**. Normalized distribution of the relative lengths of the neurites under different conditions.

## 5 Conclusion and discussion

We present a tracing algorithm designed for a high-throughput screen experiment to quantitatively analyze the neurites in fluorescence microscopy images. Based on the segmented image, we differentiate the cell body and neurites using the morphology opening operation. Our tracing algorithm can successfully trace and measure the neurites. The information on a cell-by-cell basis, such as neurite lengths and neurite complexity, can be easily extracted from the tracing results. We compared our measurement of neurite lengths with the semi-automated approach NeuronJ and a commercial software HCA-Vision. The results of the three approaches have no significant difference. Our software package is fully automatic and freely available online at *http://neuroncyto.bii.a-star.edu.sg/*. Lastly, we applied our tracing algorithm to our data set and our measurements show that the cells will have long neurites under Condition III.

## References


1. E. Meijering, M. Jacob, J.-C.F. Sarria, P. Steiner, H. Hirling & M. Unser "Design and Validation of a Tool for Neurite Tracing and Analysis in Fluorescence Microscopy Images", *Cytometry Part A* **58A**, pp. 167-176, 2004.
2. P. Madeline, T. Joachim, B.O. Amit & E.F. Alyson "NeuriteTracer: A novel ImageJ plugin for automated quantification of neurite outgrowth", *Journal of Neuroscience Methods* **168**, pp. 134–139, 2008.
3. P. Vallotton, R. Lagerstrom, C.Sun, M Buckley,D. Wang, M. D. Silva, S-S Tan & J. M. Gunnersen "Automated Analysis of Neurite Branching in Cultured Cortical Neurons Using HCA-Vision", *Cytometry Part A* **71A**, pp. 889-895, 2007.
4. O. Al-Kofahi, R.J. Radke, B. Roysam & G. Banker "Automated semantic analysis of changes in image sequences of neurons in culture", *IEEE Transaction on Biomedical Engineering* **53**, pp. 1109–23, 2006.
5. G. Xiong, X. Zhou, A. Degterev, L. Ji & S.T. Wong "Automated neurite labeling and analysis in fluorescence microscopy images", *Cytometry Part A* **69**, pp. 494–505, 2006.
6. Y. Zhang, X. Zhou, A. Degterev, M. Lipinski, D. Adjeroh, J. Yuan, *et al*. "A novel tracing algorithm for high throughput imaging Screening of neuron-based assays", *Journal of Neuroscience Methods* **160**, pp. 149–62, 2007.
7. W.M. Yu, H. K Lee, S. Hariharan, W. Y. Bu & S. Ahmed "Quantitative neurite outgrowth measurement based on image segmentation with topological dependence", *Cytometry Part A* **75A**, pp. 289-297, 2009.
8. W.M. Yu, H. K Lee, S. Hariharan, W. Y. Bu & S. Ahmed, "Level set segmentation of cellular images based on topological dependence", *International Symposium on Visual Computing* (ISVC), published in *Lecture Notes in Computer Science* **5358**, pp. 540-551, 2008.
9. C.G. Rafael, E.W. Richard, "Digital image processing". Addison-Wesley Publication Company Inc.; 1993.